A Pulse-Based Integrated Communication and Control Design for Decentralized Collective Motion Coordination

Huan Gao, *Student Member, IEEE*, and Yongqiang Wang, *Senior Member, IEEE*

***Abstract*—Decentralized collective motion coordination is fundamental in systems as diverse as mobile sensor networks, swarm robotics, autonomous vehicles, and animal groups. In motion coordination, to conform to the discontinuous message exchange that can only be conducted at discrete-time instants, existing approaches addressing motion coordination usually perform continuous control design followed by discretization-based implementation. This two-stage strategy, however, can be problematic since discretization can *harm or even destabilize* the controller designed in the continuous-time domain. Inspired by pulse-based interaction in flashing fireflies and firing neurons, we propose an integrated communication and control approach for the motion coordination. The approach circumvents discretization and can guarantee the original control design performance in final implementation. Its communication only employs simple and identical pulses, which significantly reduces processing latency and communication delay compared with conventional packet-based communications. Not only can heading control be achieved in the proposed approach to coordinate the headings (orientations) of motions in a network, but also spacing control for circular motion is achievable to design the spacing between neighboring nodes (e.g., vehicles or robots).**

***Index Terms*—Collective motion, integrated communication and control, pulse-coupled oscillators.**

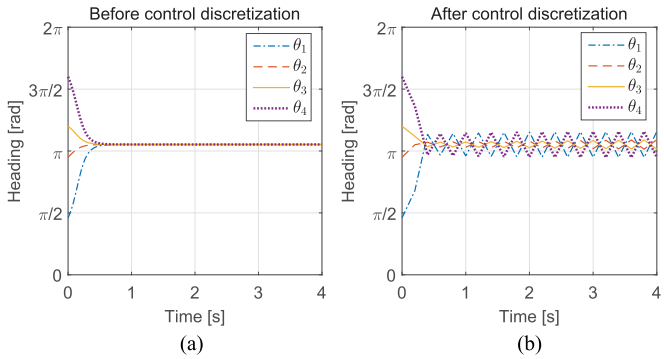

Fig. 1. Discretization destabilizes controller in [5] designed in the continuous-time domain for heading alignment. The heading control in [5] works well in the continuous-time domain assuming continuous-time information exchange (cf., (a)). However, it becomes unstable when practical communication can only occur at discrete-time instants with period 0.2 s (cf., (b), zero-order hold is used between communication). The original vehicle model in [5] was used in the implementation.

I. Introduction

An increasing number of engineering applications rely on the collective motion of a group of autonomous systems. However, most existing results on collective motion do not address the kinematic dynamics of vehicles, which hampers their practical applications. In fact, incorporating vehicle dynamics significantly increases the difficulty in decentralized collective motion coordination. Therefore, even without considering the effects of communication (e.g., discretization, message losses, time delays), early results on collective motion coordination assumed special communication patterns such as cyclic [1], [2], circulant [3], [4], or all-to-all [5]. Restricting to synchronized collective motion (aligning headings to the same value), Dimarogonas and Kyriakopoulos [6] and Moshtagh and Jadbabaie [7] proved that collective motion can be achieved under general communication patterns. Sepulchre *et al.* [8] and El-Hawwary and Maggiore [9] proved that if besides measurement information, relative estimation of global parameters can also be exchanged, then collective motion can be achieved for general communication patterns. Moshtagh *et al.* [10] further considered the situation in which only vision clues can be continuously exchanged.

All above-mentioned results are derived based on continuous exchange of information, which is key to guarantee overall continuous network dynamics and thus a simplified mathematical treatment. However, in practical implementation, information exchange between vehicles can only be conducted at discrete-time instants, making the overall dynamics much harder to address analytically. To reduce complexity, the controller design is usually performed in the continuous-time domain assuming continuous availability of neighbor's information, after which control discretization is used to conform to the actual discrete-time nature of communication. However, this approach is not appropriate in many situations, because to guarantee the design performance it usually requires a very small discretization period that leads to heavy communication burden [11]. To make things worse, discretization can *harm or even destabilize* the controller designed in the continuous-time domain [12] (cf., Fig. 1, for an example, shows that discretization can destabilize the collective motion controller in [5] designed in the continuous-time domain).

Recently, Morgansen and coauthors considered the required communication amount for cooperative control of a network of nonlinear vehicles [13], [14]. They showed that even without considering spacing control, incorporating communication effects significantly increases the complexity of heading coordination, as evidenced by the fact that analytical treatment of the splay state under all-to-all communication becomes seemingly intractable [13].

Motivated by biological pulse-coupled oscillators (e.g., flashing fireflies and firing neurons) which can achieve synchronization with remarkable robustness and simplicity through exchanging simple identical pulses at discrete-time instants, we design a pulse-based integrated communication and control approach for motion coordina-

Manuscript received June 5, 2017; accepted October 9, 2017. Date of publication October 23, 2017; date of current version May 23, 2018. This work was supported in part by the National Science Foundation under Grant 1738902. Recommended by Associate Editor Z. Ding. *(Corresponding author: Yongqiang Wang.)*

The authors are with the Department of Electrical and Computer Engineering, Clemson University, Clemson, SC 29634 USA (e-mail: hgao2@clemson.edu; yongqiw@clemson.edu).

Color versions of one or more of the figures in this paper are available online at http://ieeexplore.ieee.org.

Digital Object Identifier 10.1109/TAC.2017.2765279

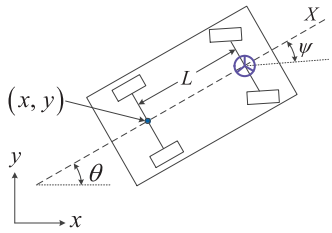

Fig. 2. Car-like vehicle model.

tion by exploiting the close relationship between phase dynamics in pulse-coupled oscillators and the heading dynamics of connected vehicles/robots. Not only does the proposed unified approach offer a natural solution for communication pattern design, it also circumvents the problem of discretization and thus guarantees achieving original design performance in final implementation.

II. Problem Formulation

Since the focus is not to control a single vehicle, but rather a vehicle network, we use a simplified vehicle model, i.e., a car-like vehicle [15], [16], to guarantee that the network dynamics is amenable to analytical treatment. The model has been widely used to model nonholonomic vehicles such as cars, boats, planes, whose controllable degrees of freedom are less than the total degrees of freedom. As illustrated in Fig. 2, the dynamics of the car-like vehicle model is given by [15]

$$\begin{cases} \dot{x} = v\cos\theta, \quad \dot{y} = v\sin\theta \\ \dot{\theta} = \dfrac{v}{L}\tan\psi \end{cases} \tag{1}$$

where (x, y) denotes the position of the midpoint of the rear axle in the two-dimensional (2-D) Euclidean plane, $\theta \in \mathbb{S}^1$ denotes the heading of the vehicle relative to the x-axis in the Euclidean plane where $\mathbb{S}^1$ is the 1-D torus, v is the speed, L is the wheelbase, and ψ is the angle of the front wheels relative to the vehicle's X-axle.

In this vehicle model, there are two control inputs v and ψ. It is worth noting that in many collective motions, vehicles/robots are usually configured to have constant velocities. For example, two most widely studied vehicles in collective motion, i.e., unmanned aerial vehicles and autonomous underwater vehicles, have constant velocities because the former must maintain a constant air speed to remain aloft [17] and the latter have a constant speed (relative to the flow field) due to effective operation requirements [18]. Therefore, in this paper, vehicles are configured to have a constant velocity $v = 1$ and ψ is used to control collective motion. Using a complex variable $r = x + \mathrm{i}y \in \mathbb{C} \approx \mathbb{R}^2$ to represent the position of the midpoint of the rear axle (which will be abbreviated as the position of the vehicle in the rest of this paper), the dynamics of a network of N vehicles is given by

$$\begin{cases} \dot{r}_k = e^{\mathrm{i}\theta_k} \\ \dot{\theta}_k = \dfrac{1}{L}\tan\psi_k = u_k \end{cases} \quad k = 1, \ldots, N \tag{2}$$

where the subscript "k" represents vehicle k, $e^{\mathrm{i}\theta_k} = \cos\theta_k + \mathrm{i}\sin\theta_k$ represents the velocity of vehicle k, and u_k denotes the curvature control (normal to vehicle heading, a.k.a. steering control) of vehicle k. From (1) and (2), the relationship between u_k and ψ_k can be obtained as $\psi_k = \arctan(L \cdot u_k)$ for $k = 1, \ldots, N$. For ease of analysis, we focus on the design of u_k, from which ψ_k can be obtained. Next, we design u_k in a decentralized manner so that desired relationships on both vehicle headings and spacing can be achieved. We first study two heading relationships, the synchronized-state and the splay-state collective motions [1], [5], based on which we address the spacing control for circular motions.

Definition 1: The synchronized-state collective motion is achieved when all vehicles/robots have the same heading, i.e., $\theta_1 = \theta_2 = \cdots = \theta_N$.

Definition 2: The splay-state collective motion is achieved when the headings are uniformly spread apart (with equal distance between heading-adjacent vehicles/robots) in the phase space $\mathbb{S}^1$. In other words, when a network of N vehicles/robots achieve the splay-state collective motion, the heading difference between any two heading-adjacent vehicles/robots is $\frac{2\pi}{N}$.

Remark 1: In many results on collective motion or oscillator networks, the splay state is also called the "balanced state" and is defined as a state on which the headings (phases) satisfy $\sum_{k=1}^{N}\sin\theta_k = \sum_{k=1}^{N}\cos\theta_k = 0$ [5]. This definition cannot guarantee equal phase distance between two heading-adjacent nodes. Therefore, our Definition 2 is more stringent.

Next, we introduce two indices for the synchronized-state and the splay-state collective motions, respectively. We first introduce an index to measure the degree of achievement of the synchronized-state collective motion

$$P_{\mathrm{syn}} \triangleq \frac{1}{N}\sum_{k=1}^{N} e^{\mathrm{i}\theta_k}. \tag{3}$$

In addition, P_{syn} is also called order parameter in oscillator network study [19]. In the synchronized-state collective motion, when all headings are identical, the magnitude (absolute value) of P_{syn} reaches its maximum ($|P_{\mathrm{syn}}| = 1$).

Using the dynamics of r_k in (2), we have $P_{\mathrm{syn}} = \frac{1}{N}\sum_{k=1}^{N}\dot{r}_k$. Therefore, P_{syn} also measures the average linear momentum of a vehicle/robot network. In the synchronized-state collective motion, because the magnitude of P_{syn} reaches the maximal value, the average linear momentum of the vehicle/robot network also reaches the maximum.

Next, we introduce a new index to measure the degree of achievement of the splay-state collective motion. Without loss of generality, we suppose that the indices of vehicle/robot headings are arranged in a way such that $\theta_1 \geq \theta_2 \geq \cdots \geq \theta_N$ holds. Then the differences between neighboring headings are given by $\Delta_k = \theta_k - \theta_{k+1}$ for $k = 1, \ldots, N-1$ and $\Delta_N = \theta_N - \theta_1 + 2\pi$. Based on which we define the index measuring the degree of achievement of the splay-state collective motion

$$P_{\mathrm{spl}} \triangleq \sum_{k=1}^{N}\left|\Delta_k - \frac{2\pi}{N}\right|. \tag{4}$$

When the splay-state collective motion is achieved, the phase differences between neighboring headings are $\frac{2\pi}{N}$ and P_{spl} in (4) will reach its minimum 0. It can also be easily verified that P_{spl} equals 0 only in the splay-state collective motion.

To simplify the design, similar to [20], we separate the control law u_k of vehicle k in (2) into two parts

$$u_k = u_k^{\mathrm{orien}} + u_k^{\mathrm{space}}. \tag{5}$$

The first part u_k^{orien} controls the heading of vehicle k. To achieve a collective motion, it should depend on the heading value of vehicle k and the time instants when vehicle k receives pulses from its neighbors. The second part u_k^{space} controls the spacing (distance) among vehicles and depends on the relative position of vehicle k with respect to its neighbors, which can be obtained by measuring the angle-of-arrival and power degradation of received pulses [17] or by using ranging and bearing sensors. In this paper, we assume all-to-all communication.

III. Integrated Communication and Control Framework for Collective Motion

Noticing that vehicle headings are similar to oscillator phases as they both evolve in the 1-D torus $\mathbb{S}^1$, we propose an integrated communication and control framework based on our study of pulse-coupled oscillators [21]–[25]. Pulse-coupled oscillators can synchronize/desynchronize oscillating phases via exchanging simple identical pulses. Inspired by the pulse-based interaction mechanism, we develop a pulse-based collective motion framework that achieves desired heading relationship via exchanging simple identical pulses. As the pulses are content free, they can be implemented at the low layer of the protocol stack (even exclusively at the physical layer) with very short message lengths, which significantly reduces the high-layer processing latencies and channel communication delays. In this framework, the time instants for pulse exchanging are determined by vehicle dynamics, so communication and control are integrated. Compared with conventional approaches using continuous control design followed by discretization-based implementation and communication, the proposed approach designs communication time instants explicitly and circumvents the problem of discretization, which in turn can guarantee that the original control design performance is attainable in final implementation.

Next we first present the idea of pulse-coupled oscillators in Section III-A, based on which we propose an integrated communication and control framework in Section III-B. The detailed design will be addressed in Sections IV and V.

A. Pulse-Coupled Oscillators

In a network of N pulse-coupled oscillators with the all-to-all communication pattern, each oscillator has a phase variable ϕ_k ($k = 1, 2, \ldots, N$) evolving continuously from 0 to 2π with a constant speed determined by its natural frequency ω_o. When the phase of an oscillator reaches 2π, this oscillator fires, i.e., emits a pulse, and simultaneously resets its phase to 0. Then the same process repeats. When an oscillator receives a pulse from its neighbor, it updates its phase according to the phase response function $P(\phi_k)$, which is defined as follows.

Definition 3: Phase response function $P(\phi_k)$ is defined as the phase shift (or jump) induced by a pulse as a function of phase at which the pulse is received [26].

The interaction mechanism of pulse-coupled oscillators can be described as follows.

1) Each oscillator has a phase variable $\phi_k \in \mathbb{S}^1$ with initial value set to $\phi_k(0)$. ϕ_k evolves continuously from 0 to 2π with a constant speed determined by ω_o.
2) When the phase variable ϕ_k of oscillator k reaches 2π, this oscillator fires, i.e., emits a pulse, and simultaneously resets ϕ_k to 0. Then the same process repeats.
3) When oscillator k receives a pulse from others, it updates its phase according to the phase response function $P(\phi_k)$

$$\phi_k^+ = \phi_k + P(\phi_k) \tag{6}$$

where ϕ_k^+ and ϕ_k denote the phases of oscillator k immediately after and before receiving the pulse. Therefore, the dynamics of oscillator k can be written as

$$\dot{\phi}_k = \omega_o + \sum_{1\le j\le N, j\neq k} P(\phi_k)\delta(t - t_j) \tag{7}$$

where t_j denotes the time instants at which ϕ_j reaches 2π. The Dirac function $\delta(t)$ is 0 for all time t except $t = 0$ and satisfies $\int_{-\infty}^{\infty}\delta(t)dt = 1$ [25].

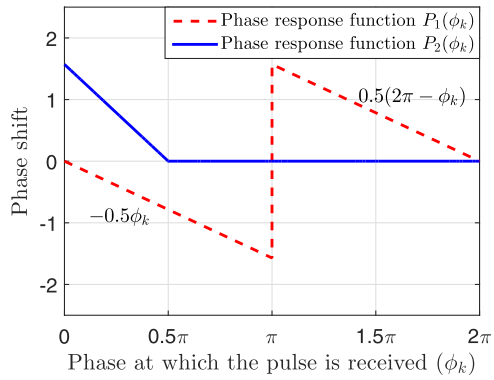

Fig. 3. Examples of phase response function that can achieve the synchronized state (red dashed line) and the splay state (blue solid line).

It is already known that if the phase response function is chosen appropriately, pulse-coupled oscillators can exhibit desired collective behaviors. For example, our results in [25] and [27] show that under phase response functions $P_1(\phi_k)$ and $P_2(\phi_k)$ in Fig. 3, oscillator phases can achieve the synchronized state and splay state, respectively.

B. Pulse-Based Collective Motion Coordination Framework

Inspired by pulse-coupled oscillators, we propose a pulse-based motion coordination framework as follows.

1) Besides heading variable θ_k and position variable r_k in (2), each vehicle also has an auxiliary variable $\phi_k \in \mathbb{S}^1$ with initial value set to $\theta_k(0)$. ϕ_k evolves continuously from 0 to 2π with a constant speed ω_o.
2) When the auxiliary variable ϕ_k of vehicle k reaches 2π, the vehicle sends a pulse, and simultaneously resets ϕ_k to 0. Then the same process repeats.
3) When a vehicle receives a pulse from its neighbor, it updates its auxiliary variable ϕ_k according to a control function $F(\phi_k, \mathbf{r})$. Note that $\mathbf{r} = [r_1, \ldots, r_N]^T$ needs to be taken into account in control design $F(\bullet)$ when spacing needs to be coordinated. The update can be mathematically formulated as follows:

$$\dot{\phi}_k = \omega_o + \sum_{1\le j\le N, j\neq k} F(\phi_k, \mathbf{r})\delta(t - t_j) \tag{8}$$

where t_j denotes the time instants at which ϕ_j reaches 2π.
4) The control input u_k for each vehicle is determined by its auxiliary variable ϕ_k by

$$u_k = \dot{\theta}_k = \omega_c + \dot{\phi}_k - \omega_o = \omega_c + \sum_{1\le j\le N, j\neq k} F(\phi_k, \mathbf{r})\delta(t - t_j) \tag{9}$$

where ω_c should be set to 0 in a rectilinear motion and the desired angular velocity in a circular motion (angular velocity ω_c corresponds to radius $\frac{1}{\omega_c}$ in circular motions).

Remark 2: The relationship between the dynamics of θ_k and the dynamics of ϕ_k can be written as

$$\dot{\theta}_k = \omega_c + \dot{\phi}_k - \omega_o \tag{10}$$

where the oscillator's natural frequency ω_o is subtracted from the dynamics of ϕ_k because the dynamics of θ_k depends on the discrete-time update $F(\phi_k, \mathbf{r})$ of ϕ_k instead of its continuous evolution, and ω_c can be seen as a part of u_k^{space} since it only affects the motion pattern (i.e., rectilinear or circular motion).

It is worth noting that in the above framework, the communicated messages are simple identical pulses and the communication time in-

stants are determined by t_j, which are determined by the evolution of ϕ_k. As ϕ_k is in turn determined by $F(\phi_k, \mathbf{r})$, the control law, the above-mentioned framework gives an integrated design of communication and control. The integrated design circumvents the effects of discretization and can guarantee that the design performance of control can be retained in final implementation. This is a great advantage over existing approaches using a continuous-domain control design followed by discretization-based implementation, which can harm or even destabilize the originally designed controller [12] (cf., Fig. 1). Furthermore, the design utilizes the analogy between phases in oscillator networks and headings in vehicle networks, which enables the treatment of nonlinear nonholonomic vehicle dynamics in (2). This is different from most event-triggered design for the collective motion of multi-agent systems that only addresses linear dynamics due to difficulties in designing a stabilizing event-triggered control. In addition, the pulse-based communication embeds information in the timing rather than the content of exchanged messages, which falls within the pulse position modulation framework in communication.

Remark 3: In the proposed integrated communication and control framework, ω_o is a design parameter controlling communication frequency. A larger ω_o leads to a higher communication frequency.

Next, we give a solution to design $F(\phi_k, \mathbf{r})$. For any vehicle k, its control $F(\phi_k, \mathbf{r})$ is not only a function of its auxiliary variable ϕ_k, but also a function of the positions of all vehicles $\mathbf{r}$. This makes $F(\phi_k, \mathbf{r})$ very difficult to derive directly, if at all possible. Given this, similar to [20] we use the singularly perturbed theory [28] to enforce a time-scale separation between the heading dynamics θ_k and the spacing dynamics r_k. We first decompose $F(\phi_k, \mathbf{r})$ into two parts as follows:

$$F(\phi_k, \mathbf{r}) = \tilde{u}_k^{\text{orien}} + \tilde{u}_k^{\text{space}}. \tag{11}$$

Then according to (5), (9), and (11), u_k^{orien} and u_k^{space} are

$$\begin{cases} u_k^{\text{orien}} &= \sum_{1\le j\le N, j\neq k} \tilde{u}_k^{\text{orien}} \delta(t-t_j) \\ u_k^{\text{space}} &= \omega_c + \sum_{1\le j\le N, j\neq k} \tilde{u}_k^{\text{space}} \delta(t-t_j). \end{cases} \tag{12}$$

Based on the singularly perturbed theory, the separation between the heading dynamics and the spacing dynamics is achievable by designing the steering control u_k as follows:

$$\begin{aligned} u_k &= K u_k^{\text{orien}} + u_k^{\text{space}} \\ &= \omega_c + \sum_{1\le j\le N, j\neq k} (K\tilde{u}_k^{\text{orien}} + \tilde{u}_k^{\text{space}}) \delta(t-t_j) \end{aligned} \tag{13}$$

where K can be set to any large value to achieve time-scale separation (make overall dynamics singularly perturbed [28]).

Combining (2) and (13) gives

$$\begin{cases} \dot{r}_k &= e^{\mathrm{i}\theta_k} \\ \epsilon\dot{\theta}_k &= \epsilon\omega_c + \sum_{1\le j\le N, j\neq k} (\tilde{u}_k^{\text{orien}} + \epsilon\tilde{u}_k^{\text{space}}) \delta(t-t_j) \end{cases} \tag{14}$$

for $1 \le k \le N$ where $\epsilon = \frac{1}{K}$ is very small so that a time-scale separation between fast dynamics in time-scale $\tau = \frac{t-t_0}{\epsilon}$ and slow dynamics in time-scale t occurs.

The position variable r_k is almost invariant in the fast time-scale τ, consequently the kinematic model can be reduced to

$$\frac{d}{d\tau}\theta_k = \epsilon\omega_c + \sum_{1\le j\le N, j\neq k} (\tilde{u}_k^{\text{orien}} + \epsilon\tilde{u}_k^{\text{space}}) \delta(t-t_j). \tag{15}$$

When K approaches infinity, ϵ approaches 0, leading to

$$\frac{d}{d\tau}\theta_k = \sum_{1\le j\le N, j\neq k} \tilde{u}_k^{\text{orien}} \delta(t-t_j). \tag{16}$$

It is clear that using the singularly perturbed control strategy, the fast dynamics of heading θ_k is decoupled from the slow dynamics of position r_k. Therefore, we can first design $\tilde{u}_k^{\text{orien}}$ to achieve the desired heading relationship, then under the heading relationship we can design $\tilde{u}_k^{\text{space}}$ to achieve the desired spacing. Since spacing control is in the slow time-scale, it will not affect the achieved heading relationship.

IV. Design of the Heading Dynamics

Note that the heading dynamics in (16) is similar to the dynamics of phases in pulse-coupled oscillators [25]. So taking inspiration from results on pulse-coupled synchronization [21], [23], [25] and desynchronization [27], we propose the following heading control strategy for the synchronized-state and splay-state collective motions, respectively.

Theorem 1: For a network of vehicles with dynamics given in (2) and initial headings constrained in a half cycle of $\mathbb{S}^1$, the vehicle headings will achieve the synchronized-state collective motion if the heading control $\tilde{u}_k^{\text{orien}}$ in (13) is given by

$$\tilde{u}_k^{\text{orien}} = \begin{cases} -l\phi_k, & 0 \le \phi_k \le \pi \\ l(2\pi - \phi_k), & \pi < \phi_k \le 2\pi \end{cases} \quad \text{for } 0 < l < 1. \tag{17}$$

Moreover, with initial headings randomly chosen from $[0, 2\pi)$ and no two vehicles having equal initial headings, the vehicle headings will achieve the splay-state collective motion if $\tilde{u}_k^{\text{orien}}$ in (13) is given by

$$\tilde{u}_k^{\text{orien}} = \begin{cases} -l\left(\phi_k - \dfrac{2\pi}{N}\right), & 0 \le \phi_k < \frac{2\pi}{N} \\ 0, & \frac{2\pi}{N} \le \phi_k \le 2\pi \end{cases} \quad \text{for } 0 < l < 1. \tag{18}$$

Proof: From the fast heading dynamics in (16) under the singularly perturbed control framework, we have $\dot{\theta}_k = \dot{\phi}_k - \omega_o$. This is different from (10) because ω_c is a part of u_k^{space} in (12) and hence will not show up in the fast time-scale dynamics (16). Further taking into account the fact that the initial value of ϕ_k is set to $\theta_k(0)$, we have $\theta_k = (\phi_k - \omega_o t) \bmod 2\pi$ for $1 \le k \le N$. Therefore, in order to prove that the headings $\theta_1, \theta_2, \ldots, \theta_N$ achieve the synchronized/splay state, we only need to prove that $\phi_1, \phi_2, \ldots, \phi_N$ achieve the synchronized/splay state.

Under the singularly perturbed control framework, the dynamics of θ_k follows (16), so ϕ_k evolves according to

$$\dot{\phi}_k = \omega_o + \dot{\theta}_k = \omega_o + \sum_{1\le j\le N, j\neq k} \tilde{u}_k^{\text{orien}} \delta(t-t_j). \tag{19}$$

Note that $\tilde{u}_k^{\text{orien}}$ in (17) and (18) is the same as the respective phase response functions $P_1(\phi_k)$ and $P_2(\phi_k)$ in Fig. 3. Therefore, the dynamics in (19) is exactly the oscillator dynamics in (7). According to the study [21], [23], [25], $\phi_1, \phi_2, \ldots, \phi_N$ will achieve the synchronized state under control (17) with initial phases constrained in a half cycle of $\mathbb{S}^1$. Therefore, $\theta_1, \theta_2, \ldots, \theta_N$ will achieve the synchronized state under control (17). Similarly, according to [27], $\phi_1, \phi_2, \ldots, \phi_N$ will achieve the splay state under control (18) when initial phases are distinct and randomly chosen from $[0, 2\pi)$. Therefore, $\theta_1, \theta_2, \ldots, \theta_N$ will achieve the splay state under control (18). ■

Next, we use simulation results to demonstrate Theorem 1. We consider the fast time-scale dynamics (16) of a network of four vehicles. Communication occurs whenever ϕ_k reaches 2π (which happens repeatedly). The control is applied when a pulse is received. We considered both rectilinear motion ($\omega_c = 0$ rad/s) and circular motion ($\omega_c = 1$ rad/s) and simulated their behavior under the different heading controls (17) and (18), respectively. ω_o is set to 10π.

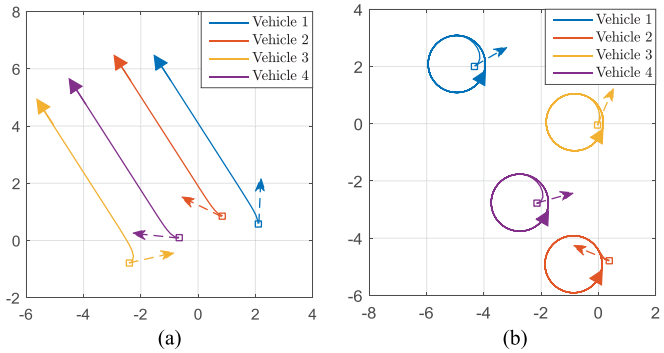

Fig. 4. Vehicle trajectories of the synchronized-state collective motion: (a) rectilinear motion case ($\omega_c = 0$ rad/s); (b) circular motion case ($\omega_c = 1$ rad/s). The initial headings, starting points, and ending points are represented by dashed arrows, squares, and solid arrows, respectively.

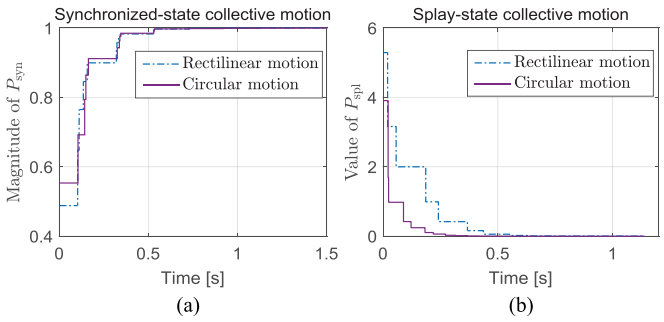

Fig. 5. (a) Magnitude of $P_{\rm syn}$ of the rectilinear motion case ($\omega_c = 0$ rad/s) and circular motion case ($\omega_c = 1$ rad/s) under the synchronized-state collective motion. (b) Value of $P_{\rm spl}$ of the rectilinear motion case ($\omega_c = 0$ rad/s) and circular motion case ($\omega_c = 1$ rad/s) under the splay-state collective motion.

We first evaluated the effectiveness of the heading control (17). The initial headings are randomly chosen from $[0, \pi)$. The vehicle trajectories of the rectilinear motion case and the circular motion case are given in Fig. 4. Also, the evolutions of the index $P_{\rm syn}$ in the two cases are given in Fig. 5(a). It can be seen that the heading control (17) can synchronize the headings of all vehicles.

Effectiveness of the heading control (18) in achieving the splay state was also evaluated. The initial headings are randomly chosen from $[0, 2\pi)$. The vehicle trajectories of the rectilinear motion case and the circular motion case are given in Fig. 6. The evolutions of index $P_{\rm spl}$ in the two cases are given in Fig. 5(b). It can be seen that the splay-state collective motion can be achieved under the heading control (18).

Remark 4: The control in (17) requires instantaneous jumps in the heading angle, which may not be desirable in certain scenarios. Fortunately, according to our recent work [29] on pulse-coupled oscillators with guaranteed phase continuity, we can use a continuous-heading-implementation mechanism to spread the needed heading adjustment in a certain time interval without affecting the convergence stability: In implementation, instead of finishing all required heading adjustment $\Delta\theta_k$ at time instant t_j, i.e., $u(t) = \Delta\theta\delta(t - t_j)$, we can spread the adjustment in a half period $T/2$ with T given by $T = 2\pi/\omega_o$, i.e., $u(t) = 2\Delta\theta_k/T$ for $t \in (t_j, t_j + T/2)$. If vehicle k has not yet achieved its desired amount of heading adjustment before a new pulse arrives (i.e., rather than having adjusted the whole amount $\Delta\theta_k$, it has adjusted only a portion of $\Delta\theta_k$), then vehicle k will use the current value of ϕ_k at the time when the new pulse is received to redetermine the value for $\Delta\theta_k$ according to (17), and evenly spread the new adjustment in the following time interval $T/2$. Under the continuous-heading-implementation mechanism, the synchronized-state collective motion can still be achieved [29].

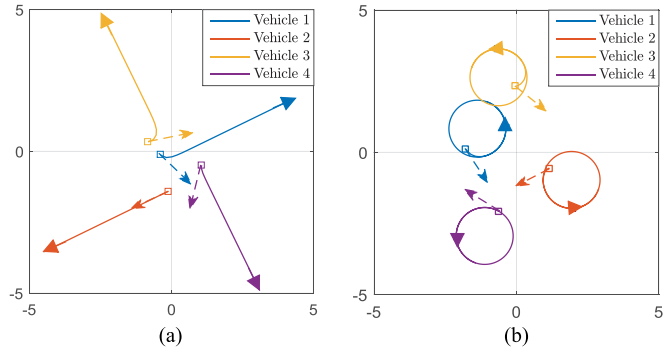

Fig. 6. Vehicle trajectories of the splay-state collective motion: (a) rectilinear motion case ($\omega_c = 0$ rad/s); (b) circular motion case ($\omega_c = 1$ rad/s). The initial headings, starting points, and ending points are represented by dashed arrows, squares, and solid arrows, respectively.

V. Stabilization of Circular Motion

Theorem 1 provides an approach to driving vehicle headings to the splay state by designing $\tilde{u}_k^{\rm orien}$ in (13). Splay-state collective motion is usually employed when vehicles perform circular motions in applications such as mobile sensor deployment [18]. In such applications, to maximize the information intake, it is usually also required that the vehicles (e.g., unmanned underwater vehicles) rotate around the same center [18]. Next, we discuss how to design the spacing control $\tilde{u}_k^{\rm space}$ to stabilize the circular motion around the centroid $R = \frac{1}{N}\sum_{k=1}^{N} r_k$.

When vehicle headings reach the splay state, the centroid $R = \frac{1}{N}\sum_{k=1}^{N} r_k$ is fixed because all headings are uniformly spread apart in the phase space $\mathbb{S}^1$ and the linear momentum satisfies $\dot{R} = \frac{1}{N}\sum_{k=1}^{N} e^{{\rm i}\theta_k} = 0$. The relative position between vehicle k and the centroid R is determined by $\tilde{r}_k = r_k - R$. Setting ω_c in (13) to the value of desired angular velocity, we can design the spacing control $\tilde{u}_k^{\rm space}$ in the following form:

$$\begin{aligned}\tilde{u}_k^{\rm space} &= \langle \omega_c \tilde{r}_k, e^{{\rm i}\theta_k} \rangle = \langle \omega_c (r_k - R), e^{{\rm i}\theta_k} \rangle \\ &= \frac{1}{N}\sum_{j=1}^{N} \langle \omega_c (r_k - r_j), e^{{\rm i}\theta_k} \rangle \end{aligned} \tag{20}$$

and thus $\tilde{u}_k^{\rm space}$ enforces the heading to be orthogonal to $\tilde{r}_k$. Noting that the absolute heading is assumed to be measurable using a digital compass (magnetometer).

Theorem 2: Under splay-state heading control (18), spacing control (20) in the singularly perturbed control framework (13) will drive all vehicles to orbit around the centroid $R = \frac{1}{N}\sum_{k=1}^{N} r_k$ with a desired angular velocity ω_c.

Proof: The center of vehicle k's circular motion is

$$c_k = r_k + {\rm i}\omega_c^{-1} e^{{\rm i}\theta_k}. \tag{21}$$

Following [5], define the Lyapunov function as $U = \frac{1}{2} \parallel \mathbf{Hc} \parallel^2$ where $\mathbf{H} = \mathbf{I}_N - \frac{1}{N}\mathbf{1}\mathbf{1}^T$, $\mathbf{1} = [1, 1, \ldots, 1]^T$, $\mathbf{c} = [c_1, c_2, \ldots, c_N]^T$, and $\mathbf{I}_N$ is the N-dimensional identity matrix.

When vehicles orbit around the same center, i.e., $c_1 = c_2 = \cdots = c_N$, we have $\mathbf{Hc} = \mathbf{0}$. Therefore, U reaches its minimum 0 when all vehicles orbit around the same center.

Since when the splay state is achieved, the heading control $\tilde{u}_k^{\text{orien}}$ vanishes, the dynamics of c_k is given by

$$\dot{c}_k = \dot{r}_k - \omega_c^{-1} e^{\mathrm{i}\theta_k}\dot{\theta}_k = e^{\mathrm{i}\theta_k} - \omega_c^{-1} e^{\mathrm{i}\theta_k}\Big\{\omega_c + \sum_{j\neq k}\tilde{u}_k^{\text{space}}\delta(t-t_j)\Big\}$$

$$= -\omega_c^{-1} e^{\mathrm{i}\theta_k}\sum_{j\neq k}\tilde{u}_k^{\text{space}}\delta(t-t_j). \tag{22}$$

Then the dynamics of U can be obtained as

$$\dot{U} = \langle \mathbf{Hc}, \mathbf{H}\dot{\mathbf{c}}\rangle = \sum_{k=1}^{N}\langle\, \mathbf{H}_k\mathbf{c}, \dot{c}_k\rangle$$

$$= -\sum_{k=1}^{N}\langle\, \mathbf{H}_k\mathbf{c}, \omega_c^{-1}e^{\mathrm{i}\theta_k}\rangle\Big\{\sum_{j\neq k}\tilde{u}_k^{\text{space}}\delta(t-t_j)\Big\} \tag{23}$$

where we used $\mathbf{H}^H\mathbf{H} = \mathbf{HH} = \mathbf{H}$, and $\mathbf{H}_k$ denotes the kth row of $\mathbf{H}$. $\mathbf{H}_k\mathbf{c}$ can be rewritten as

$$\mathbf{H}_k\mathbf{c} = c_k - \frac{1}{N}\mathbf{1}^T\mathbf{c} = r_k + \mathrm{i}\omega_c^{-1}e^{\mathrm{i}\theta_k} - R - \mathrm{i}\omega_c^{-1}\frac{1}{N}\sum_{j=1}^{N}e^{\mathrm{i}\theta_j}$$

$$= \tilde{r}_k + \mathrm{i}\omega_c^{-1}e^{\mathrm{i}\theta_k} \tag{24}$$

where we used $\frac{1}{N}\sum_{j=1}^{N}e^{\mathrm{i}\theta_j} = \dot{R} = 0$ (splay state is already achieved). So $\langle\, \mathbf{H}_k\mathbf{c}, \omega_c^{-1}e^{\mathrm{i}\theta_k}\rangle$ in (23) can be rewritten as

$$\langle \mathbf{H}_k\mathbf{c}, \omega_c^{-1}e^{\mathrm{i}\theta_k}\rangle = \langle \tilde{r}_k + \mathrm{i}\omega_c^{-1}e^{\mathrm{i}\theta_k}, \omega_c^{-1}e^{\mathrm{i}\theta_k}\rangle$$

$$= \langle \tilde{r}_k, \omega_c^{-1}e^{\mathrm{i}\theta_k}\rangle = \omega_c^{-2}\langle \tilde{r}_k, \omega_c e^{\mathrm{i}\theta_k}\rangle = \omega_c^{-2}\tilde{u}_k^{\text{space}}. \tag{25}$$

Therefore, (23) can be simplified as follows:

$$\dot{U} = -\sum_{k=1}^{N}\omega_c^{-2}\tilde{u}_k^{\text{space}}\Big\{\sum_{j\neq k}\tilde{u}_k^{\text{space}}\delta(t-t_j)\Big\}$$

$$= -\omega_c^{-2}\sum_{k=1}^{N}\sum_{j\neq k}(\tilde{u}_k^{\text{space}})^2\delta(t-t_j). \tag{26}$$

Thus, we have $\dot{U}\leq 0$ under the spacing control (20). According to LaSalle Invariance principle, all solutions will converge to the largest invariant set Λ where $\tilde{u}_k^{\text{space}} = \langle \omega_c\tilde{r}_k, e^{\mathrm{i}\theta_k}\rangle \equiv 0$ holds for $k = 1,\ldots,N$. Accordingly from (25), we have $\langle\, \mathbf{H}_k\mathbf{c}, \omega_c^{-1}e^{\mathrm{i}\theta_k}\rangle = \omega_c^{-2}\tilde{u}_k^{\text{space}} \equiv 0$ in the set Λ for $k = 1,\ldots,N$.

Since $\tilde{u}_k^{\text{space}} \equiv 0$ holds in set Λ, we have $\dot{c}_k = 0$ in (22) which implies that c_k is constant. Further taking into account the fact that $\tilde{u}_k^{\text{orien}}$ vanishes after achieving the splay state, we have $\dot{\theta}_k = u_k \equiv \omega_c$ for $k = 1,\ldots,N$. In the set Λ, $\mathbf{H}_k\mathbf{c}$ is constant since c_k is constant and θ_k is time varying because $\dot{\theta}_k \equiv \omega_c$ holds, so $\langle\, \mathbf{H}_k\mathbf{c}, \omega_c^{-1}e^{\mathrm{i}\theta_k}\rangle \equiv 0$ holds only if $\mathbf{H}_k\mathbf{c} \equiv 0$ for $k = 1,\ldots,N$, which means $c_1 = c_2 = \cdots = c_N$. Since splay state has been achieved, according to (21), we know that all vehicles orbit around the centroid, i.e., $c_1 = c_2 = \cdots = c_N = R$.

Therefore, under heading control (18), spacing control (20) will drive all vehicles to orbit around the centroid $R = \frac{1}{N}\sum_{k=1}^{N}r_k$ with a desired angular velocity ω_c. ■

Next, we use numerical simulations to confirm the theoretical results. We consider a network of $N = 4$ vehicles. ω_o is set to 10π. K is set to 5, l in (18) is set to 0.1, and the desired angular velocity ω_c is set to 1 rad/s. The initial positions of the vehicles are randomly chosen from the disk with radius 2 centering at the origin. The initial headings are randomly chosen from $[0,\ 2\pi)$. The simulation results are given in Fig. 7, which showed that the proposed integrated communication and control approach can indeed achieve the desired circular motion around the centroid.

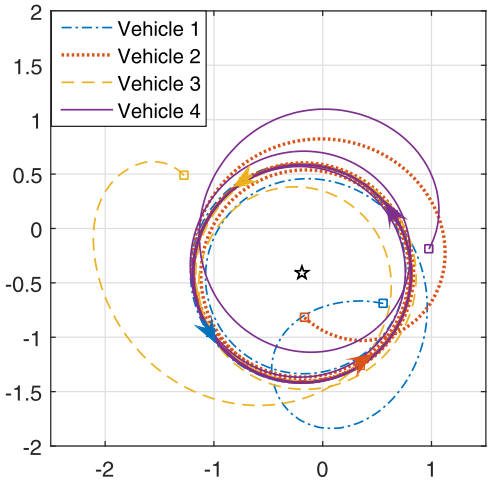

Fig. 7. Trajectories of four vehicles in circular motion around the centroid. The starting points, ending points, and final centroid are represented by squares, arrows, and a star, respectively.

VI. Conclusion

A pulse-based integrated communication and control approach is proposed for motion coordination. Different from existing results relying on a continuous control design followed by discretization-based implementation, we design communication and control in a unified framework, which can prevent the adverse effects of discretization and guarantee the design performance in implementation. The pulse-based message exchanging also significantly reduces processing latency and communication delay, and enhances robustness to channel interferences compared with conventional packet-based communication approaches.

References

[1] J. Marshall, M. Broucke, and B. Francis, "Formations of vehicles in cyclic pursuit," *IEEE Trans. Automat. Control*, vol. 49, no. 11, pp. 1963–1974, Nov. 2004.

[2] D. Paley and N. Leonard, "Collective motion of ring-coupled planar particles," in *Proc. Joint 44th IEEE Conf. Decis. Control Eur. Control Conf.*, Spain, 2005, pp. 3929–3934.

[3] D. Paley, N. Leonard, and R. Sepulchre, "Collective motion of self-propelled particles: Stabilizing symmetric formations on closed curves," in *Proc. IEEE 45th Conf. Decis. Control*, 2006, pp. 5067–5072.

[4] D. A. Paley, N. E. Leonard, and R. Sepulchre, "Stabilization of symmetric formations to motion around convex loops," *Syst. Control Lett.*, vol. 57, no. 3, pp. 209–215, 2008.

[5] R. Sepulchre, D. A. Paley, and N. E. Leonard, "Stabilization of planar collective motion: All-to-all communication," *IEEE Trans. Automat. Control*, vol. 52, no. 5, pp. 811–824, May 2007.

[6] D. V. Dimarogonas and K. J. Kyriakopoulos, "On the rendezvous problem for multiple nonholonomic agents," *IEEE Trans. Automat. Control*, vol. 52, no. 5, pp. 916–922, May 2007.

[7] N. Moshtagh and A. Jadbabaie, "Distributed geodesic control laws for flocking of nonholonomic agents," *IEEE Trans. Automat. Control*, vol. 52, no. 4, pp. 681–686, Apr. 2007.

[8] R. Sepulchre, D. A. Paley, and N. E. Leonard, "Stabilization of planar collective motion with limited communication," *IEEE Trans. Automat. Control*, vol. 53, no. 3, pp. 706–718, Apr. 2008.

[9] M. El-Hawwary and M. Maggiore, "Distributed circular formation stabilization for dynamic unicycles," *IEEE Trans. Automat. Control*, vol. 58, no. 1, pp. 149–162, Jan. 2013.

[10] N. Moshtagh, N. Michael, A. Jadbabaie, and K. Daniilidis, "Vision-based, distributed control laws for motion coordination of nonholonomic robots," *IEEE Trans. Robot.*, vol. 25, no. 4, pp. 851–860, Aug. 2009.
[11] L. Grüne, K. Worthmann, and D. Nešic, "Continuous-time controller redesign for digital implementation: A trajectory based approach," *Automatica*, vol. 44, no. 1, pp. 225–232, 2008.
[12] R. Tóth, M. Lovera, P. S. C. Heuberger, M. Corno, and P. M. J. Van den Hof, "On the discretization of linear fractional representations of lpv systems," *IEEE Trans. Control Syst. Technol.*, vol. 20, no. 6, pp. 1473–1489, Nov. 2012.
[13] D. J. Klein, P. Lee, K. A. Morgansen, and T. Javidi, "Integration of communication and control using discrete time Kuramoto models for multivehicle coordination over broadcast networks," *IEEE J. Sel. Areas Commun.*, vol. 26, no. 4, pp. 695–705, May 2008.
[14] N. D. Powel and K. A. Morgansen, "Communication-based performance bounds in nonlinear coordinated control," *Int. J. Robust Nonlinear Control*, vol. 21, no. 12, pp. 1410–1420, 2011.
[15] R. M. Murray and S. S. Sastry, "Nonholonomic motion planning: Steering using sinusoids," *IEEE Trans. Automat. Control*, vol. 38, no. 5, pp. 700–716, May 1993.
[16] F. Lamiraux and J. P. Lammond, "Smooth motion planning for car-like vehicles," *IEEE Trans. Robot. Autom.*, vol. 17, no. 4, pp. 498–501, Aug. 2001.
[17] E. W. Justh and P. S. Krishnaprasad, "Equilibria and steering laws for planar formations," *Syst. Control Lett.*, vol. 52, pp. 25–38, 2004.
[18] N. E. Leonard, D. Paley, F. Lekien, R. Sepulchre, D. M. Fratantoni, and R. Davis, "Collective motion, sensor networks, and ocean sampling," *Proc. IEEE*, vol. 95, no. 1, pp. 48–74, Jan. 2007.
[19] S. Strogatz, "From Kuramoto to Crawford: Exploring the onset of synchronization in populations of coupled oscillators," *Phys. D*, vol. 143, no. 1–4, pp. 1–20, 2000.
[20] R. Sepulchre, D. Paley, and N. Leonard, "Collective motion and oscillator synchronization," in *Cooperative Control* (2003 Block Island Workshop on Cooperative Control), V. Kumar, N. Leonard, and A. S. Morse, Eds. New York, NY, USA: Springer-Verlag, 2005, pp. 189–228.
[21] Y. Q. Wang, F. Nunez, and F. Doyle, "Energy-efficient pulse-coupled synchronization strategy design for wireless sensor networks through reduced idle listening," *IEEE Trans. Signal Process.*, vol. 60, no. 10, pp. 5293–5306, Oct. 2012.
[22] F. Nunez, Y. Q. Wang, A. R. Teel, and F. J. Doyle III, "Synchronization of pulse-coupled oscillators to a global pacemaker," *Syst. Control Lett.*, vol. 88, pp. 75–80, 2016.
[23] F. Nunez, Y. Q. Wang, and F. J. Doyle III, "Synchronization of pulse-coupled oscillators on (strongly) connected graphs," *IEEE Trans. Automat. Control*, vol. 60, no. 6, pp. 1710–1715, Jun. 2015.
[24] F. Nunez, Y. Q. Wang, and F. J. Doyle III, "Global synchronization of pulse-coupled oscillators interacting on cycle graphs," *Automatica*, vol. 52, pp. 202–209, 2015.
[25] Y. Q. Wang and F. J. Doyle III, "Optimal phase response functions for fast pulse-coupled synchronization in wireless sensor networks," *IEEE Trans. Signal Process.*, vol. 60, no. 10, pp. 5583–5588, Oct. 2012.
[26] E. Izhikevich, *Dynamical Systems in Neuroscience: The Geometry of Excitability and Bursting*. London, U.K.: MIT Press, 2007.
[27] H. Gao and Y. Q. Wang, "On phase response function based decentralized phase desynchronization," *IEEE Trans. Signal Process.*, vol. 65, no. 21, pp. 5564–5577, Nov. 2017.
[28] P. Kokotovic and H. Khalil, and J. OReilly, *Singular Perturbation Methods in Control: Analysis and Design*. Philadelphia, PA, USA: SIAM, 1999.
[29] T. Anglea and Y. Q. Wang, "Synchronization with guaranteed clock continuity using pulse-coupled oscillators." [Online]. Available: https://arxiv.org/pdf/1704.07201.pdf